AUT Journal of Mechanical Engineering

AUT J. Mech. Eng., 1(2) (2017) 233-242
DOI: 10.22060/mej.2017.12467.5345

Dynamic Response of a Red Blood Cell in Shear Flow

Z. Hashemi, M. Rahnama*

Department of Mechanical Engineering, Faculty of Engineering, Shahid Bahonar University of Kerman, Kerman, Iran

ABSTRACT: Three-dimensional simulation of a red blood cell deformation in a shear flow is performed using immersed boundary lattice Boltzmann method for the fluid flow simulation, as well as finite element method for membrane deformation. Immersed boundary method has been used to model interaction between fluid and membrane of the red blood cell. Red blood cell is modeled as a biconcave discoid capsule containing fluid with an elastic membrane. Computations are performed at relatively small and large shear rates in order to study the dynamic behavior of red blood cell, especially tumbling and swinging modes of its motion. A rigid-body-like motion with the constant-amplitude oscillation of deformation parameter and continuous rotation is observed for red blood cell at its tumbling mode. However, at a relatively large shear rate, red blood cell follows a periodic gradual deformation and elongation with a final ellipsoidal shape. The effect of different initial orientations of red blood cell is also investigated in the present paper. Results show that the dynamic response of red blood cell is not sensitive to this parameter.

Review History:

Received: 30 January 2017
Revised: 17 May 2017
Accepted: 16 July 2017
Available Online: 21 October 2017

Keywords:

Red blood cell
Three-dimensional deformation
Tumbling motion
Swinging motion

1- Introduction

Red blood cell (RBC), also known as erythrocyte, is among the most abundant cells in the blood. As a highly deformable, nucleus-free fluid-filled capsule, RBC has a complex shape similar to a biconcave disk with a larger surface area compared to that of a sphere with the same volume. RBC is capable of passing through capillaries with diameters in the order of its radius. During such movement, the membrane of RBC deforms considerably as a result of its specific property of low bending resistance. Such large deformation which, in turn, increases contact surface area with the capillary, causes more efficient exchange of Oxygen/Carbon-dioxide between RBC and its adjacent external tissues. The compromised RBC deformability contributing to human disease has also been a topic of growing research interest; diseases such as diabetes and malaria exhibit characteristic losses in RBC deformability.

Simulation of RBC deformation can be performed at different levels. A simple flow geometry consists of a shear flow with an RBC placed at its center line. Two well-known modes of RBC motion in such flow configuration are (a) tank-treading motion defined as membrane rotation around a relatively constant deformed geometry which occurs at high shear levels, and (b) tumbling motion, which is an unsteady rigid-body-like motion at small shear rates. Various experiments were carried out to reveal the details of such motions of an RBC in shear flow. Schmid-Schönbein and Wells [1], and Goldsmith and Marlow [2] were among the first researchers who studied RBC deformation in the simple shear flow experimentally and observed its tank-treading motion for the case of high shear rate and low viscosity ratio of the internal fluid to the surrounding fluid. They reported elongation of RBC toward a prolate ellipsoidal structure, aligned with the flow direction, under a shear flow. A few years later, Fischer et al. [3] and Tran-Song-Tay et al. [4] observed the same behavior in their experimental study and found that the frequency of the tank-treading mode of RBCs is related to the shear rate. Experimental findings of Pfafferott et al. [5] confirmed that when internal fluid is more viscous than its surrounding fluid, human-old-RBCs undergo tumbling motion and human-young-RBCs deform and align with the flow direction. The tumbling motion at low shear rates was also observed in the experiment of Abkarian et al. [6]. They reported another mode of motion for RBCs superimposed to tank-treading one, called swinging motion, in addition to the tumbling and tank-treading motions. The characteristics of this mode are periodic shape deformation and oscillation with inclination angle about a mean value ranging from 6º to 25º [2] while the membrane rotates around the liquid inside. In a recent experiment at a weak shear rate, Dupire et al. [7] reported that by increasing shear rate, RBC orientation changes until a steady-rolling state obtains. At moderate shear rates, RBC keeps its biconcave shape and shows a shape-preserving behavior in tank-treading/swinging regime. Simulation of spherical capsule deformation in shear flow has been done using different techniques such as boundary element method [8, 9], immersed boundary method [10-12] and immersed boundary-lattice Boltzmann method [13-15]. However, due to the complex geometry of the RBC and the numerical instabilities encountered in numerical simulations, limited research works were reported dealing with the dynamic behavior of RBCs in shear flows. There are some published papers incorporating two-dimensional simulation of a biconcave disk under shear flow [16-18]. The recent experimental, analytical, and numerical advances in the field of RBC deformation in shear flow are reviewed by Viallat

Corresponding author, E-mail: rahnama@uk.ac.ir

and Abkarian [19]. Three-dimensional simulations of RBC were reported by Eggleton and Popel [10] using immersed boundary method, and Ramanujan and Pozrikidis [8] using boundary element method. They studied the large deformation of a three-dimensional biconcave disk under shear flow. However, due to instabilities in their computations, the deformation of RBC was reported only for an initial transient period while Ramanujan and Pozrikidis [8] had reported an oscillatory behavior for the biconcave disk at later times. Unlike the spherical capsules, their results show that steady tank-treading mode is not achieved for the structures that have a non-spherical shape at rest and an oscillatory behavior as membrane rotation is expected.

Recently, in the frame work of the mesoscopic methods, there has been a hybrid method consisting of immersed boundary lattice Boltzmann method (IBLBM) and finite element method (FEM) has been used to predict flow-induced deformation of capsules [13, 20, 21]. Compared with the previous studies, it was shown that this hybrid method is capable of predicting the dynamic behavior of RBCs accurately. Sui et al. [22] studied the deformation of two-dimensional non-circular capsules with initially elliptical and biconcave shapes, as well as oblate spheroidal capsules in simple shear flow. They observed that the non-circular capsules with/without considering bending rigidity always achieve a steady tank-treading motion. The swinging and transition from swinging to tumbling motion for a biconcave discoid capsule were numerically investigated by Sui et al. [23]. Their results showed a good correspondence with the previous experimental works.

Due to the complexities of RBC deformation under shear flow, limited experimental works were published to indicate RBC motion. Tumbling and swinging motions of a red blood cell under shear flow which were reported experimentally by Abkarian et al. [6] are among those RBC's behavior which have not been fully and numerically explored. The present paper is devoted to the modeling and simulation of an RBC in a shear flow as a three-dimensional liquid-filled biconcave discoid with an elastic membrane obeying Skalak's constitutive law [24]. Using IBLBM combined with FEM, detailed behavior of RBC under a shear flow is studied with the possibility of revealing tumbling and swinging motions of a red blood cell under different shear conditions. The effect of different initial orientations of the RBC on these types of motions is also studied in detail.

2- Numerical Method

As an alternative to Navier-Stokes solvers, lattice Boltzmann Method (LBM) has been used for simulation of three-dimensional fluid flows, including RBC in a shear flow [13,20,21]. RBC is covered by a deformable solid membrane; its deformation can be modeled using finite element method, from which, membrane forces due to the deformation can be obtained. In order to simulate the hydrodynamic interactions between fluid and membrane, the immersed-boundary method can be used. These three methods which are used in the present study are described in more detail as follows.

2- 1- Lattice Boltzmann method

The lattice Boltzmann equation, which is a discretized form of the Boltzmann equation, with the BGK model reads as

$$f_\alpha(x+e_\alpha\delta t, t+\delta t)-f_\alpha(x,t)= -\frac{1}{\tau}[f_\alpha(x,t)-f_\alpha^{eq}(x,t)]+\delta t\, F_\alpha \quad (1)$$

It is obtained from the discretization of Boltzmann equation in phase space using second-order upwind scheme in space on a uniform mesh and a first order explicit Euler scheme in time. Here, $f_\alpha(x,t)$ is velocity distribution function in α^{th} discrete velocity direction, x is the spatial position vector, t is time, $f_\alpha^{eq}(x,t)$ is equilibrium velocity distribution function, F_α is the external force and τ is the relaxation time, which is related to the fluid viscosity as $\nu=(\tau-0.5)c_s^2\delta t$. Here c_s is the lattice speed of sound and is equal to $c/\sqrt{3}$. D3Q19 model has been employed for discretization of the velocity vector as shown in Fig. 1.

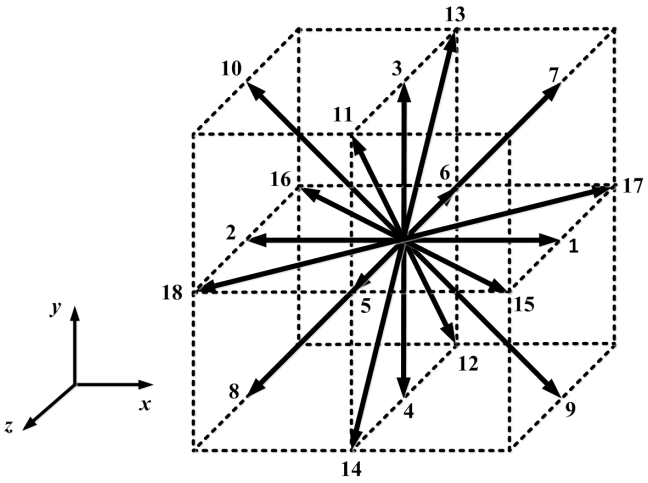

Fig. 1. D3Q19 model

Fluid particles can move in nineteen different directions in D3Q19 with discrete velocities defined as:

$$\begin{aligned} &e_0=(0,0,0)\\ &e_\alpha=(\pm1,0,0)c,(0,\pm1,0)c,(0,0,\pm1)c \qquad \alpha=1\sim6\\ &e_\alpha=(\pm1,\pm1,0)c,(0,\pm1,\pm1)c,(\pm1,0,\pm1)c \quad \alpha=7\sim18 \end{aligned} \quad (2)$$

where $c=\delta x/\delta t$ is the lattice speed. Equilibrium distribution function, $f_\alpha^{eq}(x,t)$, is obtained from:

$$f_\alpha^{eq}=\omega_\alpha\rho[1+\frac{3\vec{e}_\alpha.\vec{u}}{c^2}+\frac{9(\vec{e}_\alpha.\vec{u})^2}{2c^4}-\frac{3(\vec{u}.\vec{u})}{2c^2}] \quad (3)$$

Coefficients ω_α are weighting factors, which are defined as $\omega_0=1/3$, $\omega_\alpha=1/18$ for α = 1 to 6 and $\omega_\alpha=1/36$ for α = 7 to 18 in D3Q19 model.

External force term in LB equation can be implemented in different ways. In the present study, the proposed method of Luo [25] is used in which, the force term is added to the collision term as $F_\alpha=-3\omega_\alpha\rho e_\alpha.f/c^2$. Here f is the external force density at Eulerian nodes which is more discussed in sections 2.2 and 2.3. Knowing velocity distribution function, macroscopic variables such as density and velocity can be obtained as:

$$\rho=\sum f_\alpha \quad , \quad \rho\vec{u}=\sum\vec{e}_\alpha f_\alpha \quad (4)$$

2- 2- Membrane model

2- 2- 1- Membrane discretization

The first step in modeling membrane deformation is its discretization in the form of small elements. Here triangular elements were created on the surface of RBC membrane through mapping of a discretized spherical surface. Discretization of the sphere starts with a regular icosahedron which has 12 nodes and 20 equilateral triangles (Fig. 2(a)) and its subsequent subdivision. This approach which has been used by Ramanujan and Pozrikidis [8], Sui et al. [13] and Kruger et al. [14] is able to produce a homogeneous mesh of higher orders on a spherical membrane. Subdivision procedure consists of two steps: (a) creating additional nodes in the middle of each side of a triangle (Fig. 2(b)) and (b) radial projection of those nodes on the surface of a sphere (Fig. 2(c)).

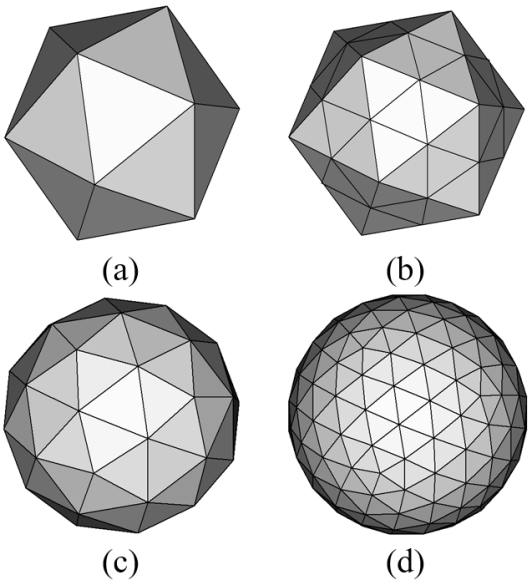

Fig. 2. Generating triangular elements on the surface of a sphere: (a) a regular icosahedron, (b) split each face of icosahedron, (c) project each new vertex on the surface of the sphere, (d) a sphere with 162 nodes/ 320 elements

This procedure is repeated until the desired resolution on the surface of the sphere is obtained (Fig. 2(d)). The number of nodes and elements cannot be selected as optional in each subdivision since the required number of nodes for Ne elements is $2N_e+2$ and the number of faces varies from $N_{e,0}=20$ (a regular icosahedron) to $N_{e,n} = 4^n N_{e,0}$ after n times of subdivision.

In order to produce red blood cells with triangular elements, one can use an appropriate mapping system from the surface of a sphere to the surface of a red blood cell. The red blood cells can be considered as a biconcave disk shape at rest that has an analytical form as [12, 26]

$$x = R_0 x', \quad y = 0.5 R_0 \sqrt{1-r^2}\left(C_0 + C_2 r^2 + C_4 r^4\right), \quad z = R \quad (5)$$

where $r^2=x'^2+y'^2$. In these equations x, y, z are the coordinates of the cell surface of an RBC, x', y', z' are the coordinates of a unit sphere, R_0 is a constant to preserve the volume, the C_i coefficients (i = 0, 2, 4) are determined experimentally as 0.207, 2.003 and -1.123, respectively. The above equations can be used as a mapping system which map each vertex on the surface of a sphere to a specific vertex on the surface of the red blood cell. The discretized surface of a sphere and a red blood cell and their cross-sections in the plane of shear are shown in Fig. 3. Fig. 3(c) shows four sample points 1, 2, 3 and 4 on the sphere which are mapped to 1′, 2′, 3′ and 4′ on the RBC, Fig. 3d.

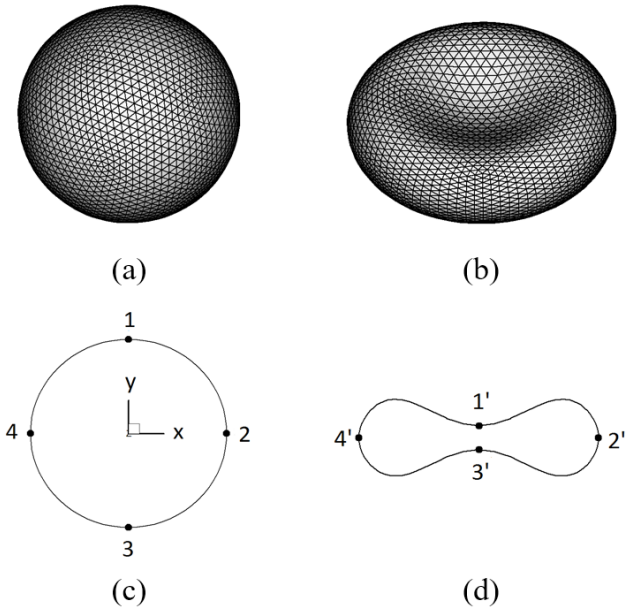

Fig. 3. The discretized surface of (a) a sphere and (b) a red blood cell. Cross-section of a (c) a sphere and (d) a red blood cell in the plane of shear and some specified vertices that are mapped

2- 2- 2- Finite element method

In the present study, the finite element method developed by Charrier et al. [27] and Shrivastava and Tang [28] is employed to find the force and deformation of each node on the surface of RBC. The main idea in their methods is that the triangular elements on the surface of the membrane are flat and remain flat even after deformation. Therefore, only the in-plane stresses are considered. In other words, undeformed and its corresponding deformed element can be represented on a plane for which, a planar deformation analysis is sufficient to obtain a deformation of the element.

One important issue in finite element analysis of RBC membrane is using an appropriate constitutive equation, which describes the membrane properties accurately. Skalak et al. [24] proposed a constitutive equation, denoted by SK, which is appropriate for describing the elastic behavior of the red blood cell. His analysis was based on the fact that a red blood cell tends to deform easily at the constant area. In this model, the resistance of membrane to area changes is represented by a coefficient C in its equation which is written as follows:

$$W^{SK} = \frac{E_s}{12}\left[\left(\lambda_1^4 + \lambda_2^4 - 2\lambda_1^2 - 2\lambda_2^2 + 2\right) + C\left(\lambda_1^2\lambda_2^2 - 1\right)^2\right] \quad (6)$$

In this equation, E_s is the surface shear elasticity modulus and λ_1 and λ_2 are the principal stretch ratios. The first term on the right-hand side of the above equation describes the shear effects and the second term represents the area dilation.

A membrane with zero change in area is obtained if C approaches infinity.

In order to determine the nodal displacements with respect to the undeformed configuration, nodal position vectors of deformed and undeformed configurations in the same plane (i.e. deformed plane) are compared based on a local coordinate system attached to elements. Using such coordinate system, local coordinate vectors, and local displacements in x and y direction (u^L, v^L) can be obtained for each vertex. The nodal forces on the vertices are obtained by using the principle of virtual work and a suitable constitutive equation (Eq. (6)):

$$\left\{F_x^L\right\} = V_e \frac{\partial W^{SK}}{\partial \lambda_1}\left\{\frac{\partial \lambda_1}{\partial u^L}\right\} + V_e \frac{\partial W^{SK}}{\partial \lambda_2}\left\{\frac{\partial \lambda_2}{\partial u^L}\right\}$$
$$\left\{F_y^L\right\} = V_e \frac{\partial W^{SK}}{\partial \lambda_1}\left\{\frac{\partial \lambda_1}{\partial v^L}\right\} + V_e \frac{\partial W^{SK}}{\partial \lambda_2}\left\{\frac{\partial \lambda_2}{\partial v^L}\right\} \quad (7)$$

where V_e is the original volume of the element. The nodal forces in local axis are transformed to the global coordinate, and the Lagrangian forces $F(s,t)$ needed in the immersed boundary method are obtained by the summation of resultant forces from all elements around the node. More details of this procedure can be found in Refs. [27, 28].

2- 3- Immersed boundary method

In general, RBC is modeled as a liquid-filled capsule surrounded by a thin elastic membrane. In order to determine the interaction between RBC and its surrounding shear flow, the immersed boundary method [29] is employed. In this method, forces exerted by the membrane are described as a distribution of regularized point forces. Considering a fixed Eulerian grid represented as 'x', conservation equations are solved for fluid inside and outside of the membrane while the membrane is tracked using Lagrangian grid points $X(s,t)$, see Fig. 4. At each time step, Lagrangian forces F(s,t) are computed at each membrane node using finite element method (section 2.2) and are distributed on the Eulerian points by the Dirac delta function interpolation:

$$f(x,t) = \sum_s F(s,t)\,\delta(x - X(s,t)) \quad (8)$$

For three-dimensional cases, the discrete delta function can be written as,

$$\delta(x - X(s,t)) = \delta(x - X(s,t))\,\delta(y - Y(s,t))\,\delta(z - Z(s,t)) \quad (9)$$

where,

$$\delta(r) = \begin{cases} 1 - |r| & |r| \le 1 \\ 0 & otherwise \end{cases} \quad (10)$$

The same interpolation function used in Eq. (8) is employed to obtain new velocities of Lagrangian nodes from the local fluid velocities, $u(x,t)$:

$$U(s,t) = \sum_x u(x,t)\,\delta(x - X(s,t)) \quad (11)$$

No-slip boundary condition is satisfied by equating membrane-node velocity with velocity obtained from its adjacent fluid nodes:

$$\frac{\partial X(s,t)}{\partial t} = u(X(s,t),t) \quad (12)$$

Using the above equation, new positions of the membrane nodes are obtained by using an explicit Euler method resulting in: $X(s,t+\Delta t)=X(s,t)+U(s,t)\Delta t$.

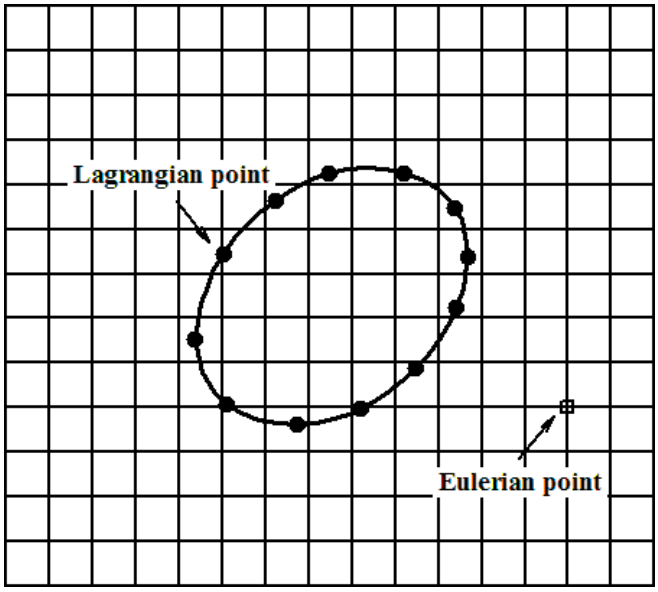

Fig. 4. Schematic diagram showing fluid Eulerian and membrane Lagrangian points

2- 4- Solution algorithm

The solution algorithm at each time step for the present combined method consists of the following steps.

1. Using initial known macroscopic fluid properties and membrane node positions, Lagrangian forces $F(s,t)$ are obtained using FEM (rf. Section 2.2).
2. Using Eq. (8), Lagrangian forces are spread to the Eulerian grids, and Eulerian force density is obtained.
3. LB equation with the Eulerian force density as a source term is solved to update flow field, section 2.1.
4. The new velocities and positions of membrane nodes are computed using Eqs. (11) and (12).
5. Computations are repeated through step 1 to reach the desired time step.

Convergence criteria were selected as having a constant value for a parameter of interest in a steady flow and corresponding values for a parameter of interest in two consecutive periods.

3- Results and Discussion

Computations are carried out to simulate an initially biconcave discoid, which can be considered as a red blood cell at rest, in the simple shear flow with velocity $\vec{V}_s=(\dot{\gamma}y,0,0)$ in which $\dot{\gamma}$ is the shear rate and y is the distance from the center of the computational domain. As shown in Fig. 5, the simulations are performed in a cubic computational domain of length 10R. R is the equivalent radius of the membrane and is defined as $R = (3V/4\pi)^{1/3}$, where V is the volume of RBC. The upper and lower solid boundaries of the computational domain move in opposite directions, while periodic boundary conditions are implemented for remaining boundaries. Unstressed RBC is located at the center of the domain with

initial inclination angle $\theta = \pi/4$ with the flow direction. A Newtonian fluid is considered to fill the entire computational domain, which covers both inside and outside of the RBC. Assuming a very thin membrane for the RBC, its bending stiffness has been neglected in the present computations. The dimensionless parameters that play important roles in membrane deformation are Reynolds number, $Re=\rho\dot{\gamma}R^2/\mu$, and dimensionless shear rate, $G=\mu\dot{\gamma}R/E_s$. Here, ρ and μ are the density and dynamic viscosity of surrounding fluid respectively. E_s is the membrane shear elasticity. Simulations are performed at low Reynolds number, which corresponds to Stokes flow regime.

Transient deformation of RBC can be measured by Taylor deformation parameter D_{xy}. As Ramanujan and Pozrikidis [8] proposed, this parameter is defined as $D_{xy}=(L_1-L_2)/(L_1+L_2)$, where L_1 and L_2 are major and minor semi-axes of RBC. Fig. 5 shows these lengths and inclination angle of RBC, θ, which is the angle between the major semi-axes and the flow direction.

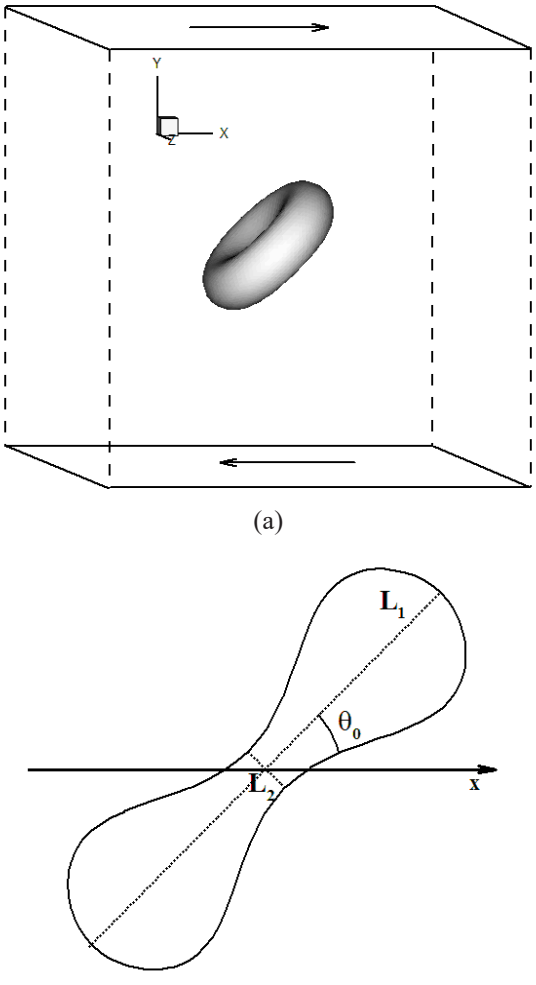

Fig. 5. (a) Schematic diagram of the computational domain, and (b) cross-section of RBC in the plane of shear with major and minor semi-axes L_1 and L_2, and inclination angle with the flow direction θ

In order to choose a membrane grid resolution with a sufficient accuracy, the time evolution of Taylor deformation parameter is computed and compared for different grid resolutions in Fig. 6. In Fig. 6, t^* is the dimensionless time defined as $\dot{\gamma}t$. The required time for one complete iteration at each resolution is also presented in Table 1. It should be mentioned that these computations were performed on a Core-i7/2.4 GHz processor. As is observed from Fig. 6, the plots of Taylor parameters nearly correspond to each other in the cases of 2562 nodes (5120 elements) and 10242 nodes (20480 elements). The discrepancy of these plots with those obtained for 162 nodes (320 elements) and 642 nodes (1280 elements) are clearly observed. On the other hand, Table 1 shows that computational time of one iteration for the case with 10242 nodes is twice the required time for the case with 2562 nodes. Therefore, a membrane grid resolution with 5120 flat triangular elements connecting 2562 membrane nodes is chosen for the present computations.

Table 1. The required time for one complete iteration in different grid resolution

Case	CPU time
320 elements, 162 nodes	0.028
1280 elements, 642 nodes	0.032
5120 elements, 2562 nodes	0.04
20480 elements, 10242 nodes	0.08

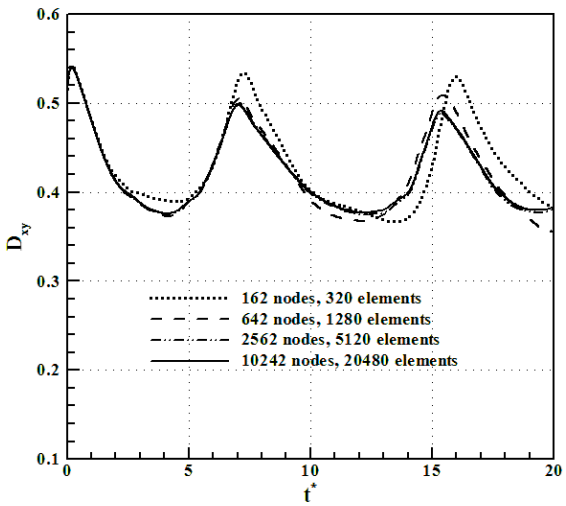

Fig. 6. Time variation of deformation parameter for different membrane grid resolutions at $G = 0.025$

3- 1- Validation

Ramanujan and Pozrikidis [8] modeled the deformation of a three-dimensional biconcave capsule using the boundary element method. However, due to the complex geometry and instabilities in their numerical computations, their results were presented for an initial short duration of time. Fig. 7 shows a comparison of Taylor deformation parameter, D_{xy}, and inclination angle, θ, versus time with those of Ramanujan and Pozrikidis [8]. A close agreement between present results and those of Ramanujan and Pozrikidis [8] reveals the accuracy of the computational method used in the present computations. Figs. 7 to 9 represent deformation parameter, inclination angle, and streamlines as well as transient deformations of an RBC at different instances for $G = 0.2$. As is observed in these figures, when RBC is exposed to shear flow, it starts

to deform and elongate while its inclination angle decreases with the flow direction. Moreover, dimples are smoothed out with time and a nearly ellipsoid shape is formed. Nodal points of the membrane would have tangential velocity after the transient initial period (no normal velocity) which makes the membrane to rotate clockwise around the interior fluid.

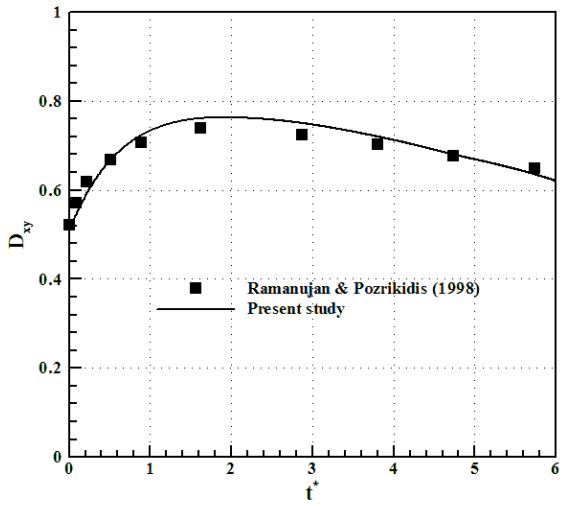

(a)

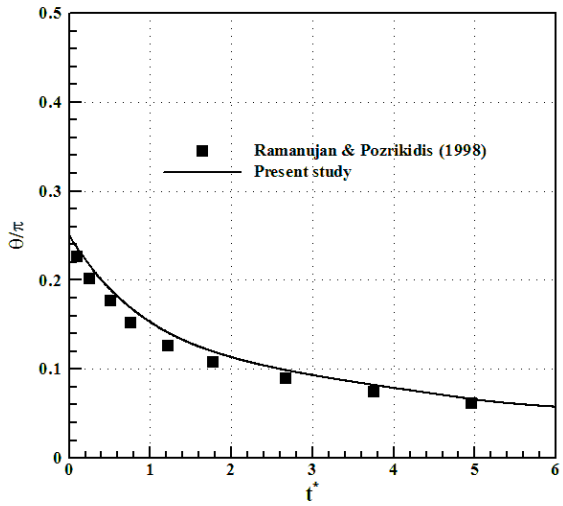

(b)

Fig. 7. Comparison of transient evolution of (a) deformation parameter and (b) inclination angle for a red blood cell in shear flow at $G = 0.2$ with the results of Ramanujan and Pozrikidis[8]

3- 2- Tumbling motion of RBC

At small shear rates, RBC undergoes an unsteady rigid-body-like motion such that it can be considered as a rigid particle rotating in a fluid. In order to study the characteristics of this type of motion, computations are repeated for low shear rates. Fig. 10 presents a temporal evaluation of inclination angle of a marker point and the deformation parameter at small dimensionless shear rates ranging from G=0.0005 to G=0.005. The deformation parameter undergoes non-decaying oscillations with a constant amplitude. At very small shear rates, i.e. G = 0.0005 to 0.001, deformation parameter is not sensitive to a variation of shear rate and RBC shows similar behaviors. As the dimensionless shear rate increases,

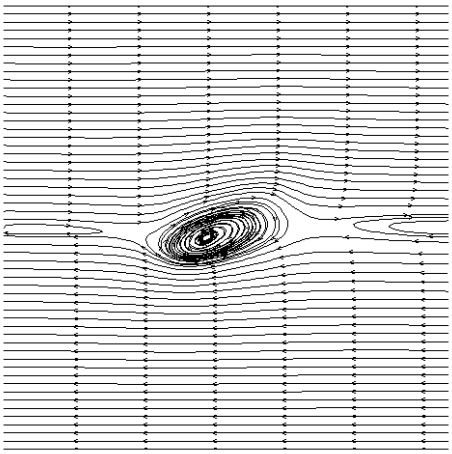

Fig. 8. Flow fields in the plane of shear around a deformed RBC for $G = 0.2$

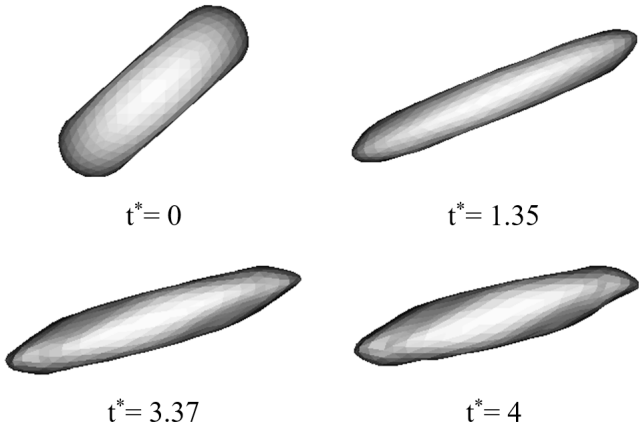

Fig. 9. Deformation of a red blood cell exposed to a simple shear flow at different times, $G = 0.2$

the amplitude of the oscillations decreases slightly.

Fig. 11 shows progressive 2D profiles of the RBC in the plane of shear with a specific marker point. The characteristics of the tumbling motion is RBC's experience of an unsteady rigid-like motion along with its continuous rotation in the clockwise direction which can be considered as the motion of a rigid particle. The 3D profiles of the RBC during the tumbling motion at G=0.0005 are represented in Fig. 12. These profiles show that RBC appears to buckle or fold slightly. This phenomenon reveals the need to implement bending stiffness of RBC despite its small value to prevent developing wrinkles on the membrane.

3- 3- Swinging motion of RBC

Swinging is another possible mode of motion for RBC in a shear flow. Based on the experimental observations of Abkarian et al. [6], RBC exposed to the shear flow experiences an unsteady mode superimposed to the tank-treading which is called swinging mode. In this case, RBC undergoes periodic shape deformation and inclination angle, while the membrane is rotating around the internal liquid. Fig. 13 shows the temporal evaluation of deformation parameter and inclination angle at large shear rates, ranging from G = 0.87 to G = 2.3. As illustrated in the figure, during this unsteady tank-treading mode, RBC experiences periodic deformation

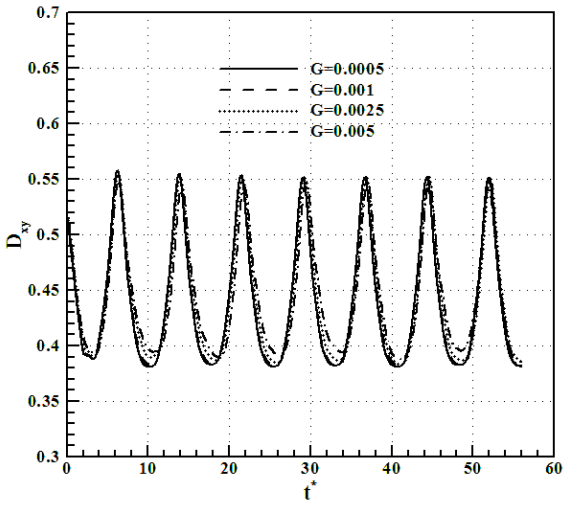

(a)

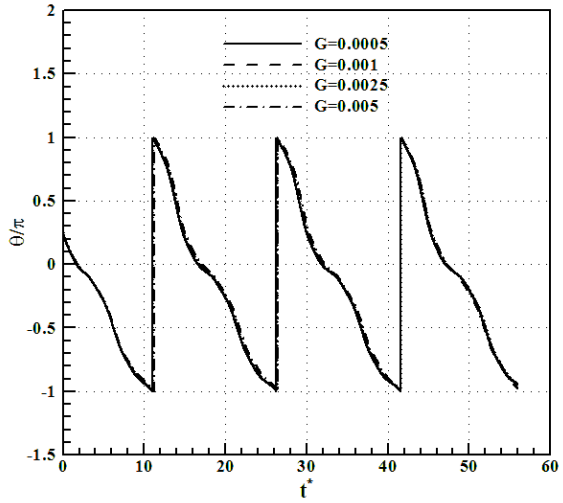

(b)

Fig. 10. Temporal evaluation of (a) deformation parameter and (b) inclination angle of a marker point at small dimensionless shear rates

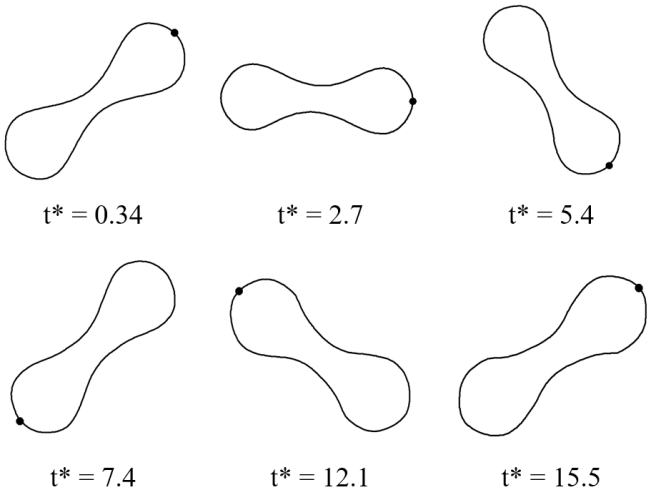

Fig. 11. RBC profiles in the plane of shear at different times during the tumbling motion, $G = 0.001$

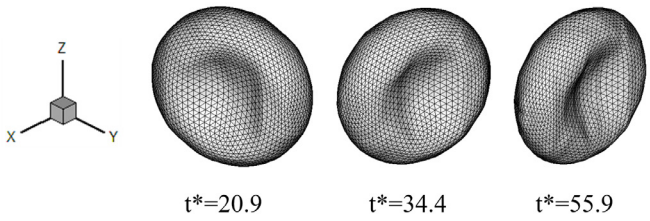

Fig. 12. 3D profiles of the red blood cell at $G = 0.0005$ and different times during tumbling

and its inclination oscillates periodically. By increasing the dimensionless shear rate, the RBC elongates more and aligns more with the flow direction.

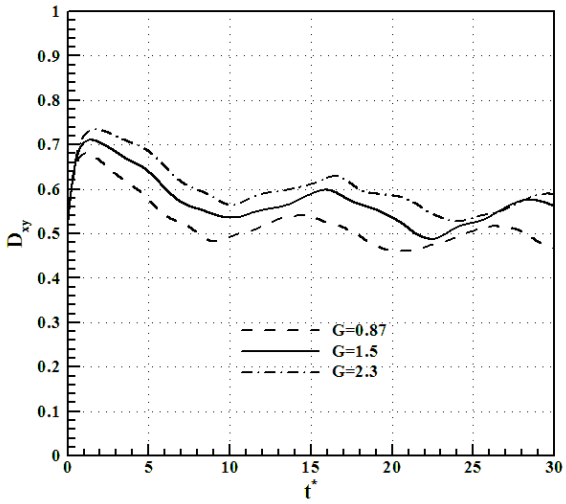

(a)

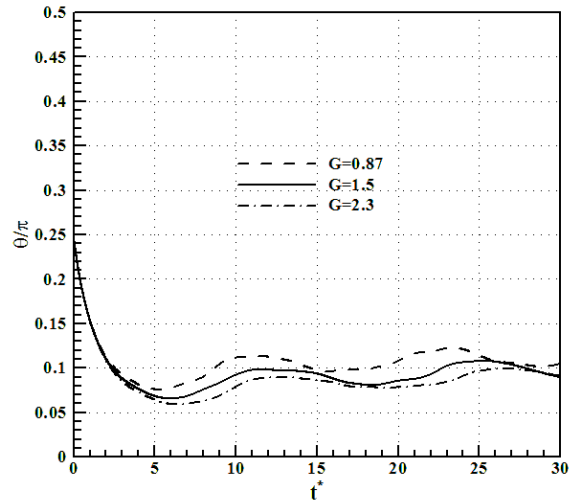

(b)

Fig. 13. Temporal evaluation of (a) deformation parameter and (b) inclination angle at large shear rates

The progressive cross-section profiles of the RBC at different planes and $G = 0.87$ are represented in Fig. 14. The RBC starts to elongate and its alignment changes. The dimples of RBC are smoothed out and an ellipsoid-like shape is obtained. The membrane rotates around the internal liquid and the material points experience unsteady tank-treading motion.

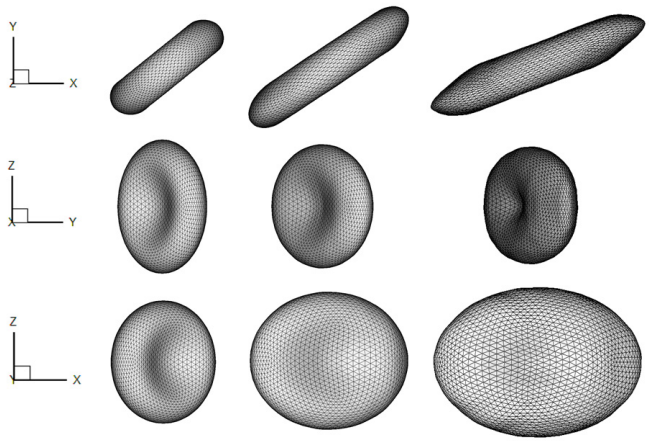

Fig. 14. Profiles of RBC at different planes in the swinging motion at $G = 0.87$ and (a) $t^* = 0.1$, (b) $t^* = 0.63$, (c) $t^* = 2.1$

3- 4- The effect of initial orientation of RBC

In order to investigate the effect of initial orientation on the RBC deformation, simulations are repeated for different initial angles with the flow direction, namely $\theta_0 = 0^\circ$ (horizontal), $\theta_0 = 45^\circ$ and $\theta_0 = 90^\circ$ (vertical). The results for $G = 0.0025$ are illustrated in Fig. 15. It is observed that initial orientation of RBC does not change the amplitude and period of oscillations of RBC significantly. Regardless of the initial orientation, RBC tends to rotate in the clockwise direction. The 3D and 2D profiles of the RBC and the marker point at different initial orientations at $t^* = 13.5$ and $G = 0.0025$ are represented in Fig. 16. Different orientation angles with the flow direction are observed at this specific time. It seems that the profiles of RBC are approximately similar to each other in spite of their difference in orientation.

4- Conclusion

In this paper, the dynamic behavior of a red blood cell in swinging and tumbling modes is studied numerically. Lattice Boltzmann method combined with the immersed boundary and finite element methods are employed to simulate three-dimensional deformable red blood cell and its interaction with the background fluid. The numerical scheme is firstly validated with the limited results of Ramanujan and Pozrikidis [8] which showed an excellent agreement for the deformation parameters, including Taylor deformation parameter and the inclination angle of the red blood cell. At small shear rates, the red blood cell tends to obtain a rigid-body-like motion and rotates continuously like a rigid particle. Under this condition, non-decaying oscillations with constant amplitude are observed in the curves of deformation parameter. However, at swinging mode, the red blood cell starts to elongate and gradually its dimples are smoothed out and deforms into an ellipsoid shape. The material points on the surface of the red blood cell rotate around the liquid inside and a periodic deformation and inclination angle is observed. It is also concluded that the present results are not sensitive to the initial orientation of the red blood cell with the flow direction.

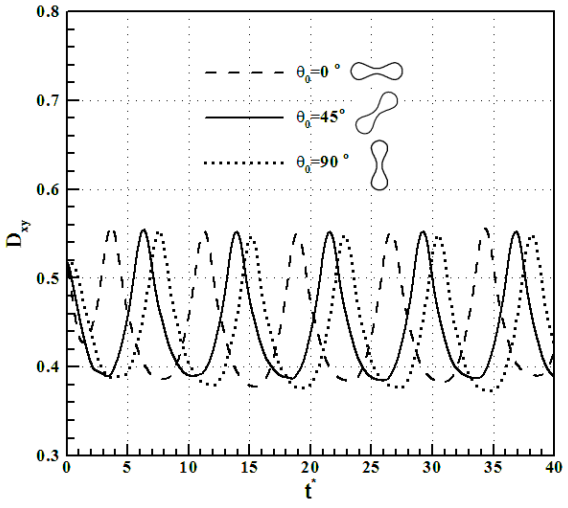

(a)

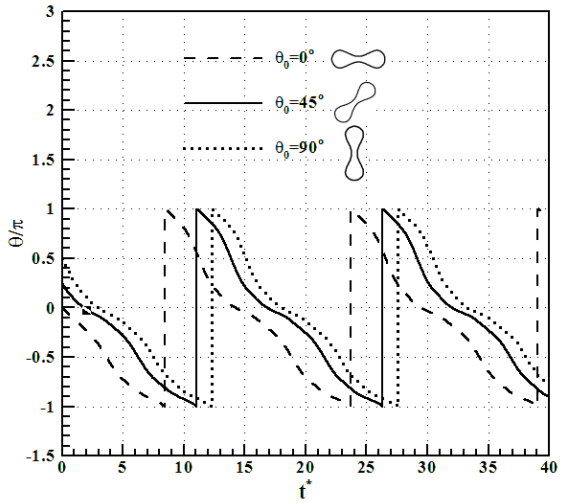

(b)

Fig. 15. The effect of different initial orientation of RBC on (a) deformation and (b) inclination, $G = 0.0025$

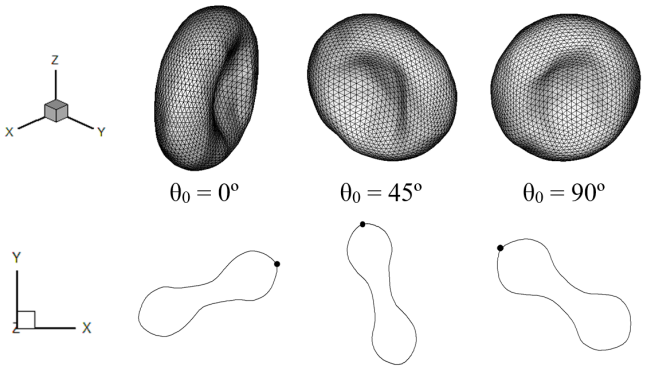

Fig. 16. 3D and 2D profiles of the red blood cell at $t^* = 13.5$ and $G=0.0025$ for initial orientations of 0°, 45°, and 90°

References

[1] H. Schmid-Schönbein, R. Wells, Fluid Drop-Like Transition of Erythrocytes under Shear, *Science*, 165(3890) (1969) 288-291.

[2] H.L. Goldsmith, J. Marlow, Flow Behaviour of Erythrocytes. I. Rotation and Deformation in Dilute

Suspensions, Proceedings of the Royal Society of London. *Series B. Biological Sciences*, 182(1068) (1972) 351-384.

[3] T.M. Fischer, M. Stohr-Lissen, H. Schmid-Schonbein, The red cell as a fluid droplet: tank tread-like motion of the human erythrocyte membrane in shear flow, *Science*, 202(4370) (1978) 894-896.

[4] R. Tran-Son-Tay, S.P. Sutera, P.R. Rao, Determination of red blood cell membrane viscosity from rheoscopic observations of tank-treading motion, *Biophysical Journal*, 46(1) (1984) 65-72.

[5] C. Pfafferott, G.B. Nash, H.J. Meiselman, Red blood cell deformation in shear flow. Effects of internal and external phase viscosity and of in vivo aging, *Biophysical Journal*, 47(5) (1985) 695-704.

[6] M. Abkarian, M. Faivre, A. Viallat, Swinging of Red Blood Cells under Shear Flow, *Physical Review Letters*, 98(18) (2007) 188302.

[7] J. Dupire, M. Socol, A. Viallat, Full dynamics of a red blood cell in shear flow, *Proceedings of the National Academy of Sciences*, 109(51) (2012) 20808-20813.

[8] S. Ramanujan, C. Pozrikidis, Deformation of liquid capsules enclosed by elastic membranes in simple shear flow: large deformations and the effect of fluid viscosities, *Journal of Fluid Mechanics*, 361 (1998) 117-143.

[9] E. Lac, Barth, Egrave, D. S-Biesel, N.A. Pelekasis, J. Tsamopoulos, Spherical capsules in three-dimensional unbounded Stokes flows: effect of the membrane constitutive law and onset of buckling, *Journal of Fluid Mechanics*, 516 (2004) 303-334.

[10] C.D. Eggleton, A.S. Popel, Large deformation of red blood cell ghosts in a simple shear flow, *Physics of Fluids*, 10(8) (1998) 1834-1845.

[11] X. Li, K. Sarkar, Front tracking simulation of deformation and buckling instability of a liquid capsule enclosed by an elastic membrane, *Journal of Computational Physics*, 227(10) (2008) 4998-5018.

[12] S.K. Doddi, P. Bagchi, Three-dimensional computational modeling of multiple deformable cells flowing in microvessels, *Physical Review E*, 79(4) (2009) 046318.

[13] Y. Sui, Y.T. Chew, P. Roy, H.T. Low, A hybrid method to study flow-induced deformation of three-dimensional capsules, *Journal of Computational Physics*, 227(12) (2008) 6351-6371.

[14] T. Kruger, F. Varnik, D. Raabe, Efficient and accurate simulations of deformable particles immersed in a fluid using a combined immersed boundary lattice Boltzmann finite element method, *Computers and Mathematics with Applications*, 61(12) (2011) 3485-3505.

[15] Z. Hashemi, M. Rahnama, S. Jafari, Lattice Boltzmann simulation of three-dimensional capsule deformation in a shear flow with different membrane constitutive laws, Scientia Iranica. *Transaction B, Mechanical Engineering*, 22(5) (2015) 1877.

[16] G. Breyiannis, C. Pozrikidis, Simple Shear Flow of Suspensions of Elastic Capsules, *Theoretical and Computational Fluid Dynamics*, 13(5) (2000) 327-347.

[17] P. Bagchi, P.C. Johnson, A.S. Popel, Computational fluid dynamic simulation of aggregation of deformable cells in a shear flow, *Journal of Biomechanical Engineering*, 127(7) (2005) 1070-1080.

[18] Y. Sui, Y.T. Chew, P. Roy, X.B. Chen, H.T. Low, Transient deformation of elastic capsules in shear flow: Effect of membrane bending stiffness, *Physical Review E*, 75(6) (2007) 066301.

[19] A. Viallat, M. Abkarian, Red blood cell: from its mechanics to its motion in shear flow, *International journal of laboratory hematology*, 36(3) (2014) 237-243.

[20] Z. Hashemi, M. Rahnama, Numerical simulation of transient dynamic behavior of healthy and hardened red blood cells in microcapillary flow, *International journal for numerical methods in biomedical engineering*, 32(11) (2016) e02763.

[21] Z. Hashemi, M. Rahnama, S. Jafari, Lattice Boltzmann simulation of healthy and defective red blood cell settling in blood plasma, *Journal of biomechanical engineering*, 138(5) (2016) 051002.

[22] Y. Sui, X. Chen, Y. Chew, P. Roy, H. Low, Numerical simulation of capsule deformation in simple shear flow, *Computers & Fluids*, 39(2) (2010) 242-250.

[23] Y. Sui, Y. Chew, P. Roy, Y. Cheng, H. Low, Dynamic motion of red blood cells in simple shear flow, *Physics of Fluids*, 20(11) (2008) 112106.

[24] R. Skalak, A. Tozeren, R.P. Zarda, S. Chien, Strain Energy Function of Red Blood Cell Membranes, *Biophysical Journal*, 13(3) (1973) 245-264.

[25] L.-S. Luo, *Lattice-gas automata and lattice boltzmann equations for two-dimensional hydrodynamics*, Ph.D. thesis, Georgia Institute of Technology, (1993).

[26] E. Evans, Y.-C. Fung, Improved measurements of the erythrocyte geometry, *Microvascular Research*, 4(4) (1972) 335-347.

[27] J. Charrier, S. Shrivastava, R. Wu, Free and constrained inflation of elastic membranes in relation to thermoforming-non-axisymmetric problems, The

Journal of Strain Analysis for Engineering Design, 24(2) (1989) 55-74.

[28] S. Shrivastava, J. Tang, Large deformation finite element analysis of non-linear viscoelastic membranes with reference to thermoforming, *The Journal of Strain Analysis for Engineering Design*, 28(1) (1993) 31-51.

[29] C.S. Peskin, The immersed boundary method, *Acta numerica*, 11 (2002) 479-517.

Please cite this article using:

Z. Hashemi and M. Rahnama, Dynamic Response of a Red Blood Cell in Shear Flow, *AUT J. Mech. Eng.*, 1(2) (2017) 233-242.

DOI: 10.22060/mej.2017.12467.5345